An Energy Adaptive Demodulation for High Data Rates with Impulse Radio

Stéphane Paquelet [1], Louis-Marie Aubert [1,2]

[1] Mitsubishi ITE-TCL, Rennes, France – [2] IETR-INSA, Rennes, France – {paquelet, aubert}@tcl.ite.mee.com

***Abstract*— The purpose of this paper is to provide an operative way of achieving high data rates for Impulse Radio (IR) transmission based systems. Because applications targeted for Ultra Wide Band (UWB) are low-cost, we especially focus on simple transceiver design. To that effect, we present an original demodulation scheme adapted to a multi-band On-Off Keying (OOK) modulation.**

The receiver's novelty consists in considering only the benefit from approximative delay spread and energy level to relax channel estimation constraints. The optimum demodulation turns out to be a non-trivial energetic threshold comparison whose precise theoretical computation admits an original analytical solution proving its feasibility. The knowledge of the available energy as well as the noise level required to set the threshold is easily obtained by appropriate estimators. Finally, in addition to simple hardware architectures, numerical results show the efficiency of these techniques.

***Index Terms*— Wireless LAN, Pulse amplitude modulation, Nonlinear detection, Estimation, Frequency division multiplexing.**

I. Introduction

Considering *Ultra Wide Band* (UWB) radio link, in accordance with the American *Federal Communications Commission* (FCC) regulation, we aim at designing a simple transceiver architecture suitable for High Data Rates.

Among all the various transmission techniques using UWB labelled modulations, the efficiency of *Impulse Radio* (IR) was pointed out. Two categories of receiver strategy were then envisioned: on the one hand optimal coherent rake receivers involving perfect channel knowledge on resolved paths, see M. Z. Win & R. A. Scholtz [1], on the other hand sub-optimal incoherent receivers essentially involving energy detection and therefore relaxed channel estimation, see Y. Souilmi & R. Knopp [2].

As we here deliberately stress low-cost hardware architectures, asynchronous methods are favoured, since they require relaxed synchronization constraints.

The following development starts with an insight into the choice of an *On-Off Keying* (OOK) modulation generalized over multiple sub-bands and a channel propagation model description. Afterward the optimal demodulation problem on a particular sub-band is set. As mentioned above its specificity consists in using a prior information made of the approximative channel delay spread and the available energy level. Deriving statistical considerations, one shows the demodulation stage consists in a non-trivial energy threshold comparison. This threshold is set by a simple and original analytical expression depending on the noise and energy level, which can be easily estimated making the implementation cost-effective. In order to illustrate the potential of these principles numerical applications based on IEEE 802.15.3a are then detailed. Possible transceiver implementations involving mainly analog devices conclude the argumentation.

II. Context setting

Examining typical characteristics of a UWB channel for IR (Fig.1), indoor propagation measurements [3], [4] show typical values of delay spread T_d ranging from 30 to 150 ns with 85% of the available energy contained in up to 60 significant paths. Moreover, the signal is distorted due to antennas and material propagation. The key idea lies in taking advantage of this natural diversity without adding complexity. For the sake of simplicity, we are thus encouraged to favour non-coherent receivers [2], working as energy integrators, rather than rake structures [1], whose practical design involves a great number of fingers.

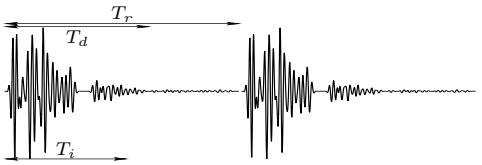

Fig. 1. Repetition time, delay spread and integration time.

An appropriate modulation for such receiver structures happens to be OOK, with a symbol repetition period T_r chosen higher than T_d to avoid inter-symbol interference. The system capacity is easily increased by duplicating this basic scheme over multiple sub-bands (from 8 to 24 bands of width $B \approx 250 - 500$ MHz).

For a given sub-band of width B, the transmitted signal is:

$$s(t) = \sum_{n=-\infty}^{+\infty} \eta_n \, p(t - nT_r)$$

where $\eta_n \in \{0, 1\}$ are the emitted bits, $p(t)$ is a pulse waveform.

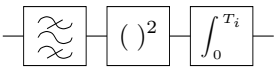

Fig. 2. Non-coherent receiver: energy integration time T_i

On the receiver side, the quadratic detector is shown on figure 2 where T_i is the energy integration time devoted to one bit demodulation.

We adopt for the received signal NLOS IEEE 802.15.3 multipath channel models [3] with additive gaussian noise $w(t)$ (two-sided spectral density $N/2$).

III. Analysis

Focusing on a particular sub-band, the demodulation stage exacts to face the two equidistributed hypotheses:

$$\begin{cases} H_0: \quad x = \displaystyle\int_0^{T_i} [n(t)]^2\, dt & \text{(bit 0)} \\ H_1: \quad x = \displaystyle\int_0^{T_i} [s_{\text{rec}}(t) + n(t)]^2\, dt & \text{(bit 1)} \end{cases}$$

where $s_{\text{rec}}(t)$ is the deterministic part of the received signal while $n(t)$ corresponds to the noise $w(t)$, each of them filtered in the appropriate sub-band.

With respect to the integrator's output x, the demodulation stage consists in deciding "at best" between H_0 and H_1, *i.e* intending to minimize the error probability.

For a given radio link, the signal's energy $E = \int_0^{T_i} s_{\text{rec}}^2(t)dt$ is fixed and can be estimated. A way to achieve this estimation is detailed in the next part.

The decision problem benefits from this knowledge to lead to the optimal rule:

$$x \underset{H_0}{\overset{H_1}{\gtrless}} \rho_{\text{opt}}$$

where the original threshold ρ_{opt} is the solution of $p_0(x) = p_1(x)$ assuming equal likely bits 0 and 1, the $p_i(x)$ being the probability density function (*pdf*) under the hypothesis $(H_i)_{i\in\{0,1\}}$.

These *pdf* are shown to be central (resp. non-central) Chi-square distribution (χ^2) for H_0 (resp. H_1) (see [5]):

$$\begin{cases} p_0(x) = \dfrac{1}{N\Gamma(M)} \left(\dfrac{x}{N}\right)^{M-1} \exp\left(-\dfrac{x}{N}\right) \\ p_1(x) = \dfrac{1}{N} \left(\dfrac{x}{E}\right)^{\frac{M-1}{2}} \exp\left(-\dfrac{x+E}{N}\right) I_{M-1}\left(2\dfrac{\sqrt{xE}}{N}\right) \end{cases}$$

where $M = BT_i$, Γ denotes the Euler function and I_n the n^{th} Bessel function of the first kind.

Finally, the threshold is found to satisfy (see [6]):

$$\frac{\rho_{\text{opt}}}{N} = \frac{E/N}{4} + M + \sqrt{M-1}\,\phi(E/N)$$

ϕ being a tabulated function depending on the variable E/N alone.

IV. Estimation of N and E

As a major improvement on usual non-coherent approaches the use of the estimation of N and E, in addition to B and T_i, enriches the *a priori* channel knowledge. A first estimation of these quantities can be achieved during a preamble step known by the receiver and sent by the transmitter after the synchronization acquisition. Then, a recursive algorithm can be implemented to refine the estimation of N and track the variation of E and then adapt the threshold's value to its optimum throughout the communication.

A. Initial estimation

During the preamble step, we extract a random vector under hypothesis H_0, $X_0 = (x_{0,1}, \cdots, x_{0,m_0})$, the components of which are m_0 independent random variables following the *pdf* $p_0(x_{0,i})$. An unbiased and efficient estimator is given by the maximum likelihood (ML) method, leading to:

$$\hat{N} = \frac{\sum_{i=1}^{m_0} x_{0,i}}{m_0 M}$$

where m_0 is the number of samples under H_0 used to estimate N.

The variance of this estimator is given by $\sigma^2_{\hat{N}} = \frac{N^2}{m_0 M}$. Assuming a gaussian distribution for the estimate $\hat{N}$ (central limit theorem for large m_0) and $M = 10$, a number of 740 samples yields an estimation of N whose relative error is below 3 % with a probabilty of 0.99.

Under the hypothesis H_1, the random vector is $X_1 = (x_{1,1}, \cdots, x_{1,m_1})$ whose elements are m_1 independent random variables following the *pdf* $p_1(x_{1,i})$. This time, the ML estimator of E can't be derived analytically. However, a simple unbiased estimator can be obtained by the moments method. Using only the mean value of x under H_1: $E_1[x] = MN + E$ which can be simply estimated by $\frac{1}{m_1}\sum_{i=1}^{m_1} x_i$, we easily derive the following estimator of E:

$$\hat{E} = \frac{\sum_{i=1}^{m_1} x_{1,i}}{m_1} - M\hat{N}$$

where m_1 is the number of samples under H_1 used to estimate E.

The variance of this estimator is $\sigma^2_{\hat{E}} = \frac{MN^2+2EN}{m_1} + M^2\sigma^2_{\hat{N}}$. With values corresponding to a worst case ($M = 10$, $E/N =$ 13 dB and $m_0 = 740$), a number of 1230 samples yields an estimation of E whose relative error is below 3 % with a probabilty of 0.99.

Finally, the preamble length $m_0 + m_1$ is about 2000 bits. With an upper bound for T_r equal to 100 ns the time allocated to estimate N and E doesn't exceed 0.2 ms.

B. Recursive estimation

To refine the estimation of N and E during the demodulation step, we seek a real time algorithm in which the estimate at rank $m+1$ is expressed according to the estimate at rank m and the new sample x_{m+1}.

Concerning the estimation of N, this can be achieved by the ML recursive algorithm given by:

$$\hat{N}_{m_0+1} = \hat{N}_{m_0} + \Delta N_{m_0}$$

with $\Delta N_{m_0} = \frac{I^{-1}(\hat{N}_{m_0})}{m_0+1} \frac{\partial}{\partial \hat{N}_{m_0}} \ln p_{x,0}(x_{m_0+1}, \hat{N}_{m_0})$ where $I(\hat{N}_{m_0})$ is the Fisher information equal to $\frac{M}{\hat{N}_{m_0}^2}$.

The result is straightforward:

$$\hat{N}_{m_0+1} = \frac{m_0}{m_0+1}\hat{N}_{m_0} + \frac{x_{m_0+1}}{(m_0+1)M}$$

This estimator is very simple to implement in hardware and benefit from the same properties as the ML. Its variance $\sigma^2_{\hat{N}} = \frac{N^2}{m_0 M}$ tends to zero as m_0 tends to infinity.

As for E, although the ML method can't be applied a simple recursive algorithm can be derived from the previous estimator $\hat{E}$ used during the preamble :

$$\hat{E}_{m_1+1} = \frac{m_1}{m_1+1}\hat{E}_{m_1} + \frac{x_{m_1+1} - M\hat{N}}{m_1+1}$$

However, the value of E may change during the demodulation step. In the above recursive estimator, when m_1 is large the new sample x_{m_1+1} becomes insignificant and the estimate $\hat{E}_{m_1+1}$ is maintain whatever the variations of the real value of E. To track these variations the gain $\frac{1}{m_0+1}$ of a new sample must be set to a fixed value $1/K$, which yields the recursive estimator:

$$\hat{E}_{m_1+1} = \left(1 - \frac{1}{K}\right)\hat{E}_{m_1} + \frac{x_{m_1+1} - M\hat{N}}{K}$$

For a fixed E, the variance of this estimator tends to $\frac{MN^2+2EN}{2K-1}$ as m_1 tends to infinity.

V. System performances

On FIG. 3 are plotted performances P_e versus $\mathcal{E}/N$, where $\mathcal{E} = E/2$ is the energy averaged over equiprobable bits 0 and 1, recovered by various receivers. The performances of OOK modulations are calculated with a threshold which is assumed to be optimally set (i.e. N and E are perfectly estimated).

Let's consider typical values of $M = BT_i$ between 7 and 25 and $P_e \approx 10^{-5}$. To compete with the proposed non-coherent OOK receiver, capable of integrating almost the whole available energy, a coherent BPSK rake receiver should recover at least 33% to 40% of the whole energy (4 to 5 dB difference). Taking up such a challenge with a realistic number of fingers is quite unlikely due to the propagation characteristics outlined in section I. This obviously confers an inherent advantage to the non-coherent scheme.

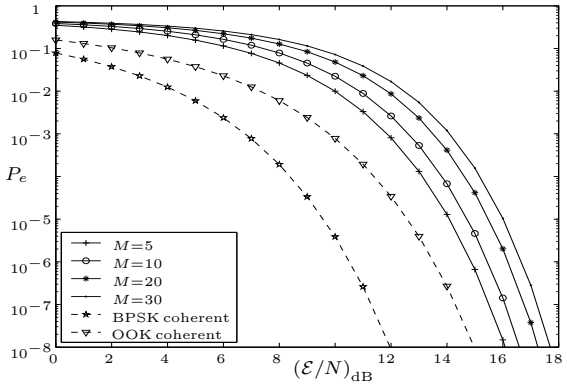

Fig. 3. Error probability versus $\mathcal{E}/N$ for different values of M.

The practical system performances are illustrated in table I (see [6] for more details), with link budgets for typical environments according to IEEE 802.15.3a channel models with respect to the FCC regulation [7]. The performances obviously match the IEEE standard requirements.

Bit rate	**150**	**240**	**600**	Mbit/s
d	**10**	**5**	**3**	m
B	500	500	250	MHz
N_{band}	12	12	24	
T_r	80	50	40	ns
CM	4	3	2	
T_i	50	40	30	ns
$\overline{P}_e$	10^{-5}	10^{-5}	10^{-5}	

TABLE I. Performances samples.

VI. Hardware implementation

The following hardware implementation (FIG. 4 and 5) greatly benefits from the relaxed constraints offered by the asynchronous approach.

Only a coarse synchronization is required, which makes the system robust against the clock jitter and every triggering inaccuracy. Moreover, since the processing is based on energy, phase non-linearities of devices like antennas, amplifiers, filters, etc. are not critical. Furthermore, due to multi-band slicing, many components have a relatively narrow working band, which simplifies their design. An interesting feature to notice here is that the architecture offers a simple power control in each sub-band. This kind of flexibility is useful to fulfill a regional power spectral density mask. This also permits to avoid a sub-band which is perturbed by an narrow-band interferer. Finally, thanks to the use of mainly analog and passive devices, a low power consumption can be achieved.

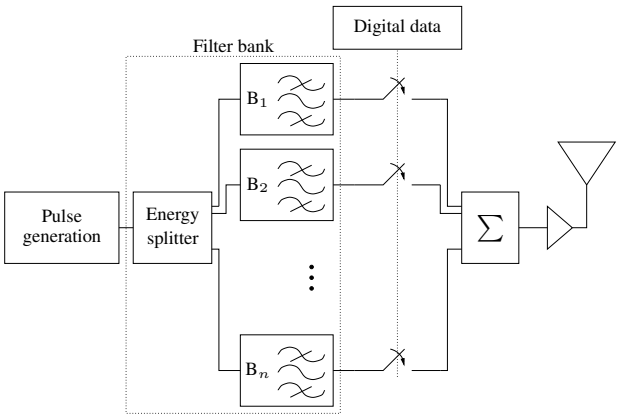

Fig. 4. Transmitter implementation sketch.

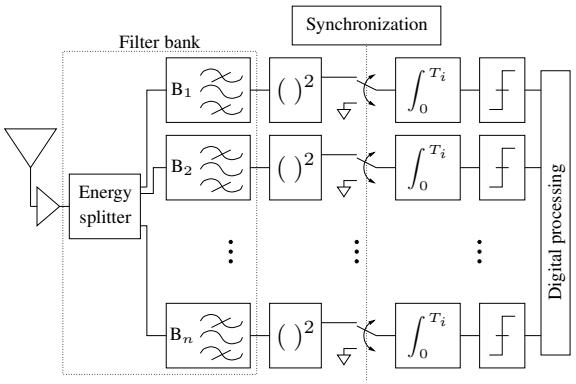

Fig. 5. Receiver implementation sketch.

To implement the functional scheme shown above, a solution based on multiple antennas is envisioned. If M antennas are used, each of them is followed by a filter bank of N filters, with $M \times N$ typically equal to 24. For example, in a realistic implementation, six antennas working in a range of 1 GHz are each followed by four filters of 250 MHz. This kind of antenna's form factor is compatible with the overall system integration. The same applies to the pulsers: each of the six pulsers feeds a splitter that distributes the energy over four filters.

The figure 6 details the sketch at the output of the square law device.

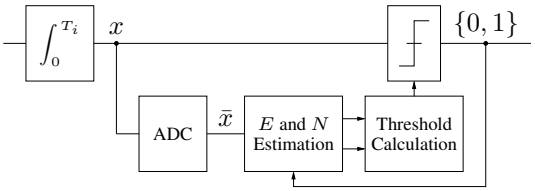

Fig. 6. Integrator's output sampling

Since the useful part of the squared signal is a lowpass signal ($f_{max} = B$ between 250 and 500 MHz), the integrator and comparator subset is the same on each sub-band. In this device, the integrator's output x is sampled at a rate of $1/Tr < 30$ MHz. An analog to digital conversion over 4 to 8 bits is used for estimating N and E. Once the threshold is set the demodulation stage doesn't require more than one bit, which allows a precise analog threshold comparison using signal x. The A/D conversion during this stage can be turned off to save power. Conversely, it can be maintain to adapt the threshold according to the channel variation. The quantized signal $\bar{x}$ also makes a soft decoding possible.

CONCLUSION

A simple non-coherent transceiver providing high data rate with impulse radio was proposed. It was shown that using a prior information made of the approximate channel delay spread and the available energy level allows the non-coherent system to reach high performances. This simple analog-oriented architecture can obsiously be capitalized for low-cost applications.

Premilinary results relating to the hardware implementation confirm the high potential of these principles. In particular, integration in small and low cost devices is easier than what could be assumed at a first glance.

Besides, relaxed synchronization methods based on asynchronous time-hopped signal detection have also been investigated to enable fast channel delay spread estimation.

From a system point of view, usual *Medium Access Control* (MAC) is currently re-visited taking benefit from energy detection techniques based on the inherent flexible frequency separation properties of such a system.

ACKNOWLEDGMENT

We wish to thank BERNARD UGUEN from IETR-INSA research laboratory who contributes to the hardware implementation schemes. We also thank CLAIRE MEUNIER who closely participated to the mathematical developments and GWILLERM FROC whose experience as a physicist encouraged us to investigate these principles.

REFERENCES

[1] Win, M.Z.; Scholtz, R.A.; "Impulse radio: how it works," *IEEE Communications Letters,* Vol. 2, No. 2, Feb. 1998, pp. 36-38.

[2] Souilmi, Y.; Knopp, R.; "Challenges in UWB signaling for adhoc networking," *DIMACS Workshop on Signal Processing for Wireless Transmission,* Oct. 2002

[3] IEEE; "Channel modeling sub-committe report," *IEEE P802.15 Wireless Personal Area Networks,* Feb. 7, 2003.

[4] Tchoffo Talom, F.; Uguen, B; Plouhinec, G. Chassay and F. Sagnard, "Study of interactions effects on Ultra WideBand signals propagation," *Proc. IEEE IWUWBS 2003 Conf.,* June 2003.

[5] Humblet, P. A.; Azizoglu, M.; "On the bit-error rate of lightwave systems with optical amplifiers," *Journal of Lightwave Technology,* vol. 9, pp. 1576-1582, Nov. 1991.

[6] Paquelet, S.; Aubert, L.-M.; Uguen, B.; "An Impulse Radio Asynchronous Transceiver for High Data Rates" *Joint UWBST Conf. & IWUWBS 2004,* May 2004.

[7] Federal Communications Commission "First report and order," *ET Docket No. 98-153,* April 22, 2002.